

September 2003, corrected January 2004  
 PM/03-18  
 THES-TP 2003/03-03.  
 hep-ph/0309032.

# Neutralino-neutralino annihilation to photon and gluon pairs in MSSM models.<sup>†</sup>

G.J. Gounaris<sup>a</sup>, J. Layssac<sup>b</sup>, P.I. Porfyriadis<sup>a</sup> and F.M. Renard<sup>b</sup>

<sup>a</sup>Department of Theoretical Physics, Aristotle University of Thessaloniki,  
 Gr-54124, Thessaloniki, Greece.

<sup>b</sup>Physique Mathématique et Théorique, UMR 5825  
 Université Montpellier II, F-34095 Montpellier Cedex 5.

## Abstract

The complete 1-loop computation of the processes  $(\tilde{\chi}_i^0 \tilde{\chi}_j^0 \leftrightarrow \gamma\gamma, gg)$ , for any pair of the four MSSM neutralinos, has been performed for an arbitrary c.m energy. As a first application suitable for Dark Matter (DM) searches, the neutralino-neutralino annihilation is studied at relative velocities  $v/c \simeq 10^{-3}$  describing the present DM distribution in the galactic halo, and  $v/c \simeq 0.5$  determining neutralino relic density contributions. Numerical results are presented for 31 MSSM benchmark models indicating considerable sensitivity to the input parameters. Numerical codes are released, which may be used for the computation of the annihilation of any two neutralinos to two photons or two gluons at the aforementioned  $v/c$  values. In the near future, we intend to complement them with codes for the inverse process  $\gamma\gamma \rightarrow \tilde{\chi}_i^0 \tilde{\chi}_j^0$ , observable at the future high energy Linear Colliders.

PACS numbers: 12.15.-y, 14.80.Ly, 95.35+d

---

<sup>†</sup>Programme d'Actions Intégrées Franco-Hellenique, Platon 04100 UM

The nature of the Dark Matter (DM), which is here assumed to be possibly sensitive only to the usual gravitational and weak forces [1, 2], is still open. At present, a most obvious candidate for such matter in the context of R-parity conserving Supersymmetric (SUSY) theories, should be the Lightest Supersymmetric Particle (LSP) [3]. In the minimal Supersymmetric models (MSSM), this is most often identified with the lightest neutralino  $\tilde{\chi}_1^0$  [4, 5]. Within MSSM there exist cases though, where the LSP is the purely gravitationally interacting gravitino, while the lightest neutralino may then appear as the next to lightest supersymmetric particle (NLSP) [6].

In any case, depending on the MSSM parameters, one or more neutralinos may sizably contribute to DM [1, 2]. Such DM could be investigated though direct or indirect methods. Direct detection could occur through *e.g.* the observation of the nucleus recoil induced by the  $\tilde{\chi}_1^0$ -nucleus scattering [7]. Experimental setups are looking for such events [8], and there even exist claims that a signal may have already been observed [9].

Indirect detection refers to searches of anomalies in the spectrum of the photons, neutrinos, positrons or antiprotons, emitted from cosmologically nearby sites, where the neutralino concentration might be enhanced [1, 2]. Both types of searches are however difficult, because of uncertainties in making precise predictions for the dark matter density distribution in these sites [10], and the strong sensitivity of the observable quantities on the SUSY parameters.

However, as noticed several years ago [11, 12], the process<sup>1</sup>  $\tilde{\chi}_1^0\tilde{\chi}_1^0 \rightarrow \gamma\gamma$  (as well as  $\tilde{\chi}_1^0\tilde{\chi}_1^0 \rightarrow \gamma Z$ ), should be particularly interesting for Dark Matter detection, since the neutralino pair annihilation is essentially taking place at rest, producing sharp monochromatic photons. Provided therefore that the cross section  $\sigma(\tilde{\chi}_1^0\tilde{\chi}_1^0 \rightarrow \gamma\gamma)$  and the neutralino concentration in the galactic halo are not very small, the signal to be searched for would be sharp photons coming from the central region of the Galaxy, with energies in the hundred-GeV region.

The companion process  $\tilde{\chi}_1^0\tilde{\chi}_1^0 \rightarrow gg$  may also be important in some regions of the parameter space, where its sufficiently frequent occurrence may modify the analyses of the neutrino and antiproton signals [13]. Furthermore, if the second neutralino  $\tilde{\chi}_2^0$  turns out to be very close to  $\tilde{\chi}_1^0$ , processes like  $(\tilde{\chi}_1^0\tilde{\chi}_2^0 \rightarrow \gamma\gamma, gg)$  and  $(\tilde{\chi}_2^0\tilde{\chi}_2^0 \rightarrow \gamma\gamma, gg)$  may also be interesting; particularly the gluonic mode may then play a role in determining the relic neutralino density and the rates of neutrino and antiproton production [13].

These statements sufficiently motivate our interest in the general processes  $\tilde{\chi}_i^0\tilde{\chi}_j^0 \leftrightarrow \gamma\gamma, gg$ , ( $i, j = 1-4$ ). The lowest order non-vanishing contribution to them arise from one loop diagrams involving standard and supersymmetric particle exchanges; *i.e.* sleptons, squarks, gauginos and additional Higgses, which sensitively depend on the precise SUSY particle spectrum, couplings and mixings. Thus, DM considerations of the processes  $(\tilde{\chi}_i^0\tilde{\chi}_j^0 \rightarrow \gamma\gamma, gg)$ , and studies of the inverse processes  $\gamma\gamma \rightarrow \tilde{\chi}_i^0\tilde{\chi}_j^0$  in a Linear Collider (LC), and  $gg \rightarrow \tilde{\chi}_i^0\tilde{\chi}_j^0$  at LHC, may provide very strong constraints on the various MSSM models.

Previous computations have only addressed the diagonal annihilation  $\tilde{\chi}_i^0\tilde{\chi}_i^0 \rightarrow \gamma\gamma, gg$

---

<sup>1</sup> $\tilde{\chi}_1^0$  denotes the lowest neutralino.

of two identical neutralinos at vanishing relative velocity [11, 12, 13]. Such approximations may of course be adequate for neutralinos annihilating at present in the galactic halo (or the Sun or Earth), where their average relative velocity is expected to be  $v/c \simeq 10^{-3}$  [1]. But this low energy limit may not be generally adequate for neutralino relic density computations, which is determined by neutralino annihilation at a time when their average relative velocity prevailing in Cosmos was  $v/c \simeq 0.5$  [1, 14].

We have, therefore, made a complete one loop computation of  $\tilde{\chi}_i^0 \tilde{\chi}_j^0 \leftrightarrow \gamma\gamma, gg$ , in a general MSSM model with real parameters, expressing all helicity amplitudes in terms of the Passarino-Veltman functions, for general incoming and outgoing momenta. The derived expressions, which should be useful in both dark matter and LC and LHC studies, are quite complicated though, so that the only efficient way to present them is through numerical codes. Details for both types of processes and applications to collider physics searches, will be given in a separate extended paper [15].

In the present paper we restrict to studies of the  $\tilde{\chi}_i^0 \tilde{\chi}_j^0 \rightarrow \gamma\gamma$  and  $\tilde{\chi}_i^0 \tilde{\chi}_j^0 \rightarrow gg$  annihilations in the framework of DM searches, where the average relative velocity  $v_{ij}$  of the two neutralinos is small. Two numerical codes, PLATONDml and PLATONDmg are released [16], which compute the neutralino annihilation cross sections times  $v_{ij}$ ; *i.e.*  $(v_{ij}/c) \cdot \sigma(\tilde{\chi}_i^0 \tilde{\chi}_j^0 \rightarrow \gamma\gamma)$  and  $(v_{ij}/c) \cdot \sigma(\tilde{\chi}_i^0 \tilde{\chi}_j^0 \rightarrow gg)$  respectively, at  $v_{ij}/c \simeq 10^{-3}$ , as it would be expected for galactic halo neutralinos at present [11, 12, 1]. In addition, a third code PLATONGrel, is also released, which calculates  $(v_{ij}/c) \cdot \sigma(\tilde{\chi}_i^0 \tilde{\chi}_j^0 \rightarrow gg)$  at  $v_{ij}/c \simeq 0.5$ , which should be useful for neutralino relic density computations. The outputs of all codes are in fb.

### Procedure.

The generic structure of the one-loop diagrams for  $\tilde{\chi}_i^0 \tilde{\chi}_j^0 \rightarrow \gamma\gamma$  in the 't-Hooft-Feynman gauge, is depicted in Fig.1, where the types of particles running clockwise inside each loop are: box (a), ( $fSSS$ ), ( $fWWW$ ), ( $fSSW$ ), ( $fSWW$ ), ( $fSWS$ ), ( $fWWS$ ); box (b), ( $Sfff$ ), ( $Wfff$ ); box (c) ( $SffS$ ), ( $WffW$ ), ( $SffW$ ), ( $WffS$ ); initial triangle (d), ( $SfS$ ), ( $WfW$ ); final triangle (e), ( $WWW$ ), ( $SSS$ ),  $SWW$ ,  $SSW$ ; final triangle (f), ( $fff$ ); and bubbles (g) ( $SS$ ), ( $WW$ ); (h).  $WS$ . By  $S$  we denote the scalar exchanges (Higgs, Goldstone and sfermions); and by  $f$  the fermionic ones (leptons, quarks and inos). Bubbles (g) and final triangles (e) and (f), are connected to the initial  $\tilde{\chi}_i^0 \tilde{\chi}_j^0$  state through an intermediate  $Z$ , or neutral Higgs or Goldstone boson  $h^0, H^0, A^0, G^0$ . For the  $\tilde{\chi}_i^0 \tilde{\chi}_j^0 \rightarrow gg$  process, only the subset of the diagrams in Fig.1, involving quark and squark loops, is needed. We also note that the  $\tilde{\chi}_i^0 \tilde{\chi}_j^0$ -antisymmetry, and the Bose symmetries of the  $\gamma\gamma$  and  $gg$  states, provide non-trivial tests for the helicity amplitudes of  $\tilde{\chi}_i^0 \tilde{\chi}_j^0 \rightarrow \gamma\gamma, gg$ , which we have checked to be satisfied [15].

### General features for small relative velocities.

When the relative velocity  $v_{ij}$  among the neutralino pairs is small, their c.m energy to order in  $(v_{ij}/c)^4$ , is

$$s = (m_i + m_j)^2 + m_i m_j \left( \frac{v_{ij}}{c} \right)^2 \left[ 1 + \left( \frac{v_{ij}}{c} \right)^2 \left( \frac{3}{4} - \frac{2m_i m_j}{(m_i + m_j)^2} \right) \right] . \quad (1)$$

For very small values of<sup>2</sup>  $v_{ij}$ , the angular distribution of  $d\sigma(\tilde{\chi}_i^0 \tilde{\chi}_j^0 \rightarrow \gamma\gamma, gg)/d\cos\theta$  is flat, and  $v_{ij}\sigma(\tilde{\chi}_i^0 \tilde{\chi}_j^0 \rightarrow \gamma\gamma, gg)$  is a smooth function of  $v_{ij}^2$ .

Since  $\sigma(\tilde{\chi}_i^0 \tilde{\chi}_j^0 \rightarrow \gamma\gamma, gg)$  are induced by 1-loop processes, the expected order of magnitude for very small  $v_{ij}/c$  is

$$\begin{aligned} v_{ij}\sigma(\tilde{\chi}_i^0 \tilde{\chi}_j^0 \rightarrow \gamma\gamma) &\simeq \frac{\alpha^4 c}{M_{eff}^2} \simeq \frac{3 \times 10^{-32} cm^3 sec^{-1}}{M_{eff}^2 (\text{TeV})} , \\ v_{ij}\sigma(\tilde{\chi}_i^0 \tilde{\chi}_j^0 \rightarrow gg) &\simeq \frac{\alpha^2 \alpha_s^2 c}{M_{eff}^2} \simeq \frac{6 \times 10^{-30} cm^3 sec^{-1}}{M_{eff}^2 (\text{TeV})} , \end{aligned} \quad (2)$$

where  $M_{eff}$  is an effective mass-scale, depending on the masses and mixings of the external neutralinos and the particles running inside the loops. For such  $v_{ij}/c$ , the two neutralinos are predominantly in a  ${}^1S_0$  state, so that only helicity amplitudes satisfying  $\lambda_1 = \lambda_2$  and  $\mu_1 = \mu_2$  are allowed.

The dominant diagrams in this case are the boxes ( $Sfff$ ), ( $SffS$ ) ( $fWWW$ ), ( $Wfff$ ), ( $WffW$ ), ( $fWGW$ ), ( $GffW$ ), ( $WffG$ ). Triangle and bubble contributions are either vanishing or numerically negligible, except for the case where the s-channel exchanged neutral Higgs is very close to the sum of the two neutralino masses; compare Fig.1e-h. In such a case, depending on whether  $\tilde{\chi}_i^0$  and  $\tilde{\chi}_j^0$  have the same or opposite CP eigenvalues, the main contribution arises from the exchange of either  $A^0$  or<sup>3</sup>  $H^0$ , respectively.

The magnitude of  $v_{ij}\sigma$  in (2), may thus be enhanced, if relatively light stops, sbottoms, and charginos or staus (for the  $\gamma\gamma$  case only) exist, and one of them happens to be almost degenerate to one of the incoming neutralinos; or if a neutral Higgs, with an appropriate CP eigenvalue, is very close to the c.m. neutralino energy, (compare the diagram of Fig.1e-h). But the most important role in determining the  $v_{ij}\sigma$ -magnitude seems to be played by the nature of the neutralino contents; mixture percentages of Wino, Higgsinos or Bino. The Wino-type neutralinos usually give the largest cross sections, followed up by the Higgsinos, while Binos are most often supplying very small cross sections. This ordering comes from the dominant role played by the box diagrams involving  $W$  bosons and the neutralino-chargino- $W$  couplings. For example, it has been emphasized that if the lightest neutralino  $\tilde{\chi}_1^0$  is Higgsino-like and close to a chargino, then  $M_{eff} \simeq m_W$ , leading to  $v\sigma(\tilde{\chi}_1^0 \tilde{\chi}_1^0 \rightarrow \gamma\gamma) \sim 10^{-28} cm^3 sec^{-1}$ , independently of the neutralino mass; compare (2), [11, 12]. We confirm this result. In fact, we have numerically checked that our exact 1-loop computation reproduces the results of [11, 12], obtained through a non-relativistic treatment of the annihilation cross section of two identical neutralinos at threshold. It should also be remarked that (2) is consistent with unitarity in our calculations, provided that the neutralino masses are in the TeV-range or below, [17]. Thus, higher order effects can be safely ignored.

### Illustrations for various MSSM models.

Using the numerical codes PLATONdml, PLATONdmg and PLATONgrel, we obtain the

<sup>2</sup>For all MSSM-models we are aware of, the differential cross section is flat for  $v_{ij}/c \lesssim 0.5$ .

<sup>3</sup>The lightest  $h^0$  is below threshold in all models considered.

results for  $v_{ij}\sigma(\tilde{\chi}_i^0\tilde{\chi}_j^0 \rightarrow \gamma\gamma)$  and  $v_{ij}\sigma(\tilde{\chi}_i^0\tilde{\chi}_j^0 \rightarrow gg)$  presented in Tables 1, 2 and 3, for an extensive set of benchmark SUSY models involving real parameters only. These models are used here just in order to indicate the range of possible results we could obtain. They all satisfy  $\mu > 0$  and have been suggested as being roughly consistent with present theoretical and experimental constraints [18, 19, 20, 21, 22]. In constructing these codes, the exact 1-loop expressions for  $\tilde{\chi}_i^0\tilde{\chi}_j^0 \rightarrow \gamma\gamma, gg$ , have been used.

In the same Tables, the grand scale parameters of the various benchmarks MSSM models are also shown. Conveniently, these models are divided into three classes:

- Universal m-SUGRA models. Apart from the  $\mu$ -sign, there exist four additional GUT scale parameters in these models, namely  $(m_{1/2}, m_0, A_0, \tan\beta)$ . They are given in the left part of Table 1. The *SPS*-models in this Table come from the Snowmass set [18], *AD(fg5)<sub>1,2</sub>* from Fig.5 of [19], and *Rosz<sub>2</sub>* from Fig.2 of [20].
- Non-universal m-SUGRA models. The grand scale parameters of these models are presented in the upper part of Table 2. In the models *AD(fg9)* (coming from Fig.9 of [19]) and *SPS6* [18],  $m_{H_u}$  is allowed to deviate at the grand scale from the scalar mass unification condition; while in the *CDG*-models, the gaugino large scale unification is violated [21].
- GMSB and AMSB models. The grand scale parameters for the gauge mediated symmetry breaking (GMSB) models (*SPS7, SPS8*), and the anomaly mediated symmetry breaking (AMSB) models *SPS9*, are given in Table 3, [18].

Using a public code like *e.g.* SuSpect [23], the electroweak scale parameters of the above benchmark models may be calculated from their grand scale values; while the also needed total widths of the supersymmetric neutral Higgs particles<sup>4</sup>  $H^0$  and  $A^0$ , are calculated using<sup>5</sup> HDECAY [24]. These in turn are used in the in-files of the three PLATON codes.

We next turn to the results for  $v_{ij}\sigma(\tilde{\chi}_i^0\tilde{\chi}_j^0 \rightarrow \gamma\gamma, gg)$  for the<sup>6</sup>  $(\tilde{\chi}_1^0\tilde{\chi}_1^0)$ ,  $(\tilde{\chi}_1^0\tilde{\chi}_2^0)$  and  $(\tilde{\chi}_2^0\tilde{\chi}_2^0)$  cases, which appear in Tables 1,2,3. Of course, the  $(\tilde{\chi}_1^0, \tilde{\chi}_1^0 \rightarrow \gamma\gamma)$  case is the most interesting one for Dark Matter detection in the halo, but the other modes (especially the gluonic ones if they turn out to be appreciable), may play an important role for the determination of the value of the DM relic density and the rates of neutrino and antiproton production [13]. Below we discuss these results, in conjunction with the electroweak scale masses and couplings of the various models.

The  $\tilde{\chi}_1^0\tilde{\chi}_1^0 \rightarrow \gamma\gamma$  mode.

In all universal mSUGRA models of Table 1,  $\tilde{\chi}_1^0$  is predominantly a Bino, which implies rather small values for  $v\sigma$ , in agreement with [11, 12]. The smallest  $v\sigma$  values, in the range

---

<sup>4</sup>Compare the diagrams in Fig.1e-h.

<sup>5</sup>In some non-universal SUSY models we are using, an HDECAY version is needed allowing independent values for the gaugino parameters  $M_1$  and  $M_2$  at the electroweak scale. We thank Abdelhak Djouadi for providing us with this code.

<sup>6</sup>Here  $(\tilde{\chi}_1^0, \tilde{\chi}_2^0)$  are the lightest and the next to lightest neutralinos.

of  $10^{-33} \text{ cm}^3 \text{sec}^{-1}$ , appear for the *SPS2* models characterized by very heavy sfermions and charginos. Such values increase to the  $10^{-31} \text{ cm}^3 \text{sec}^{-1}$  level, for the *Rosz<sub>2</sub>*, *SPS4* and *AD(fg5)<sub>2</sub>* models, where sfermions and charginos have masses of a few hundreds of GeV; and they are further enhanced to a few times  $10^{-30} \text{ cm}^3 \text{sec}^{-1}$ , in models like *SPS3<sub>1</sub>* or *SPS3<sub>2</sub>* where the lightest  $\tilde{\chi}_1^0$  is close to  $\tilde{\tau}_1$ . These enhancements remain nevertheless moderate, because the intermediate ( $\tilde{\chi}_1^0 \tilde{\chi}_1^0 \rightarrow \tau^- \tau^+$ )-contribution to the  $\tilde{\chi}_1^0 \tilde{\chi}_1^0 \rightarrow \gamma\gamma$  amplitudes is depressed by the small  $\tau$  mass.

The non-universal mSUGRA set of models (Table 2) includes cases like *AD(fg9)*, in which the  $\tilde{\chi}_1^0$  is predominantly of Higgsino-type, leading to  $v\sigma \sim 3 \times 10^{-29} \text{ cm}^3 \text{sec}^{-1}$  [11, 12]. Much larger values like  $v\sigma \sim 10^{-27} \text{ cm}^3 \text{sec}^{-1}$  are reached in the *CDG<sub>200</sub>* and *CDG<sub>OII</sub>* cases though, in which  $\tilde{\chi}_1^0$  is predominantly a Wino combined with an appreciable Higgsino component. The fact that  $\tilde{\chi}_1^+$  is rather close to  $\tilde{\chi}_1^0$  in the *AD(fg9)*, *CDG<sub>200</sub>* and *CDG<sub>OII</sub>* models, also plays a role in enhancing  $v\sigma \tilde{\chi}_1^0 \tilde{\chi}_1^0 \rightarrow \gamma\gamma$ .

In all other cases of Table 2,  $\tilde{\chi}_1^0$  is mainly a Bino and  $v\sigma$  is small. Among them, worth mentioning may be the *CDG<sub>75</sub>* model, which displays the very rare property to have a CP-odd  $\tilde{\chi}_1^0$ .

When it happens that  $m_{A_0} \simeq 2m_{\tilde{\chi}_1^0}$ , then it is very important to correctly include the  $A^0$  width, which we have done by using the code HDECAY [24]. An example of a case where the  $A^0$  width is necessary, is *CDG<sub>200</sub>*.

In Table 3, we present the results for the GMSB models (*SPS7*, *SPS8*), and the AMSB models *SPS9* [18]. In (*SPS7*, *SPS8*),  $\tilde{\chi}_1^0$  is mainly a Bino and  $v\sigma$  rather small compared to the result in the *SPS9* model where  $\tilde{\chi}_1^0$  is mainly a Wino. In (*SPS7*, *SPS8*) there exists a near degeneracy of  $\tilde{\chi}_1^0$  with  $\tilde{\tau}_1$ , which enhances the intrinsically small Bino result up to the  $10^{-29} \text{ cm}^3 \text{sec}^{-1}$  level. In *SPS9*, which is characterized by a near degeneracy of the Wino-like  $\tilde{\chi}_1^0$  with  $\tilde{\chi}_1^+$ , the enhancement is much bigger, leading to  $v\sigma \sim 10^{-27} \text{ cm}^3 \text{sec}^{-1}$ .

### The $\tilde{\chi}_1^0 \tilde{\chi}_1^0 \rightarrow gg$ mode.

In Tables 1,2,3 we give results both, for  $v/c \simeq 10^{-3}$  and  $v/c \simeq 0.5$ . As in the  $\gamma\gamma$  case, the largest  $v\sigma$  values appear for a Wino-like  $\tilde{\chi}_1^0$ , smaller ones for Higgsinos, and very small values for the Bino case. On top of this, further enhancements may occur when  $\tilde{\chi}_1^0$  is very close to  $\tilde{\tau}_1$ ; or when  $m_{A^0} \simeq 2m_{\tilde{\chi}_1^0}$  where a considerable sensitivity on  $v/c$  may also be induced, (see *e.g.* *CDG<sub>200</sub>* in Table 2).

As seen from Tables 1,2,3, the  $v\sigma$  rates vary from  $2 \times 10^{-31}$  to  $7 \times 10^{-29} \text{ cm}^3 \text{sec}^{-1}$  for the universal m-SUGRA models; from  $10^{-30}$  to  $10^{-28} \text{ cm}^3 \text{sec}^{-1}$  for the non-universal m-SUGRA models, with the exceptional case of *CDG<sub>200</sub>* giving  $\sim 10^{-26} \text{ cm}^3 \text{sec}^{-1}$ ; and from  $3 \times 10^{-31}$  to  $2 \times 10^{-29} \text{ cm}^3 \text{sec}^{-1}$  as we move from the AMSB towards the GMSB models of Table 3.

### The $\tilde{\chi}_1^0 \tilde{\chi}_2^0$ and $\tilde{\chi}_2^0 \tilde{\chi}_2^0$ annihilations.

In the  $\gamma\gamma$  case,  $v\sigma(\tilde{\chi}_1^0 \tilde{\chi}_2^0)$  is very often considerably smaller than  $v\sigma(\tilde{\chi}_1^0 \tilde{\chi}_1^0)$ , while  $v\sigma(\tilde{\chi}_2^0 \tilde{\chi}_2^0)$  considerably larger and often reaching the  $10^{-27} \text{ cm}^3 \text{sec}^{-1}$  level. This is usually driven by the fact that  $\tilde{\chi}_2^0$  is mainly a Wino in all models where  $\tilde{\chi}_1^0$  dominantly a Bino. The

occasional degeneracy of  $\tilde{\chi}_2^0$  with  $\tilde{\chi}_1^+$ , further enhances this value. The only models where the  $\tilde{\chi}_2^0\tilde{\chi}_2^0$  rate is smaller than the  $\tilde{\chi}_1^0\tilde{\chi}_1^0$  one, are  $CDG_{200}$ ,  $CDG_{OII}$  and the AMSB ones, in which the Wino component of  $\tilde{\chi}_1^0$  is usually considerably larger than that of  $\tilde{\chi}_2^0$ .

In the  $gg$  case, the  $\tilde{\chi}_1^0\tilde{\chi}_2^0$  cross sections can be either larger or smaller than the  $\tilde{\chi}_1^0\tilde{\chi}_1^0$  ones, because of the varying situations for the squark and chargino contributions, and orthogonalities that tend to appear in certain couplings. In contrast to this,  $\chi_2^0\chi_2^0$  is most often larger than  $\tilde{\chi}_1^0\tilde{\chi}_1^0$ , but the relative magnitudes are often not so large as in the  $\gamma\gamma$  case. Rates like  $v\sigma(\chi_2^0\chi_2^0) \sim 10^{-28} \text{ cm}^3\text{sec}^{-1}$  are often realized. Exceptional cases like  $SPS3_1$  and  $SPS6_3$  give  $10^{-26} \text{ cm}^3\text{sec}^{-1}$  at  $v/c \simeq 10^{-3}$ , while  $SPS6_2$  gives a similar value at  $v/c \simeq 0.5$  at least partly due to  $A^0$  resonance effects.

### Final comments.

In conclusion, we confirm that  $v_{ij}\sigma(\chi_i^0\chi_j^0 \rightarrow \gamma\gamma, gg)$  annihilation at  $v_{ij}/c \sim 10^{-3}$ , can assume a wide range of values. This arises because these processes start at one loop, thereby being sensitive to many aspects of the sfermion, ino and Higgs boson masses, and the peculiar mass-coincidences appearing in many MSSM cases.

The results should be useful for Dark Matter searches through neutralino annihilation to sharp photons. Roughly, the gamma-ray flux expected in such a case from a direction at an angle  $\psi$  with respect to the direction of the galactic center, is given by [10]

$$\frac{d\mathcal{F}}{d\cos\psi} \simeq (10^{-12} \text{ cm}^{-2}\text{s}^{-1}) \left[ \frac{v\sigma(\chi_1^0\chi_1^0 \rightarrow \gamma\gamma)}{10^{-29} \text{ cm}^3\text{s}^{-1}} \right] J(\psi), \quad (3)$$

where  $J(\psi)$  depends on the dark matter density distribution along the line of sight. Its magnitude is expected to be of order one at high  $\psi$ ; but it increases as  $\psi$  decreases, and in some models it may even reach values up to  $10^5$  when looking towards the galactic center [10]. On the basis of this, it seems that for  $v\sigma(\chi_1^0\chi_1^0 \rightarrow \gamma\gamma) \gtrsim 10^{-29} \text{ cm}^3\text{s}^{-1}$ , the observation of a sharp photon line with an energy  $E_\gamma$  precisely corresponding to the mass of the LSP  $\tilde{\chi}_1^0$ , should be possible [25]. The actual observation of such energetic photons would supply an interesting confirmation of Supersymmetry, provided of course that the actual observations would allow for acceptable values of the relic density of the lightest neutralino. In this respect, the process  $\chi_i^0\chi_j^0 \rightarrow \gamma Z$  may also be interesting, and we are planning to extend our study to it.

The neutralino relic density depends on the total annihilation cross section (summing all final states like  $f\bar{f}$ ,  $WW$ ,  $ZZ$ , ...)[2]. Concerning this, we have found that the gluonic (sometimes even the photonic channel) may be important in some models, and that occasionally considerable variations may appear in  $v_{ij}\sigma(\chi_i^0\chi_j^0 \rightarrow gg)$ , as  $v_{ij}/c$  varies between  $10^{-3}$  and 0.5. In more detail, the neutralino contribution to cold dark matter (CDM) is

$$\Omega_{CDM} \simeq \frac{6 \cdot 10^{-27} \text{ cm}^3\text{s}^{-1}}{\langle \sigma_{\text{ann}} v_{\text{rel}} \rangle} \quad (4)$$

where  $\langle \sigma_{\text{ann}} v_{\text{rel}} \rangle$  is the average total neutralino annihilation cross section multiplied by the relative velocity at  $v_{\text{rel}}/c \simeq 0.5$ . For a model to be consistent with cosmological

constraints, we expect that  $\langle \sigma_{\text{ann}} v_{\text{rel}} \rangle \sim 10^{-26} \text{cm}^3 \text{s}^{-1}$ . Thus, we note *e.g.* from Table 2 that in the  $CDG_{200}$  model, both  $v\sigma(\tilde{\chi}_1 \tilde{\chi}_1 \rightarrow gg)$  and  $v\sigma(\tilde{\chi}_1 \tilde{\chi}_1 \rightarrow \gamma\gamma)$  are of the order  $10^{-27} \text{cm}^3 \text{s}^{-1}$ . A similar situation appears for  $v\sigma(\tilde{\chi}_1 \tilde{\chi}_1 \rightarrow \gamma\gamma)$  in the AMSB Snowmass models [18] in Table 3. We are tempted to conclude therefore that it would be safer, if both these processes are included in the relic density computations.

Because of the sensitivity of the results to the SUSY models, and in order to contribute in the successive stages of the required analysis, we have started the construction of a series of numerical codes (PLATON) which will be made public so that anyone can run his preferred set of MSSM parameters or explore the parameter space. At present the codes PLATONdml allow to compute the annihilation rates  $(v_{ij}/c)\sigma(\tilde{\chi}_i^0 \tilde{\chi}_j^0 \rightarrow \gamma\gamma)$  at  $v/c \simeq 10^{-3}$ , while PLATONdmg and PLATONgrel determine  $(v_{ij}/c)\sigma(\tilde{\chi}_i^0 \tilde{\chi}_j^0 \rightarrow gg)$  at  $v/c \simeq 10^{-3}$  and  $v/c \simeq 0.5$  respectively, always in fb [16].

If the emerging overall picture turns out to be cosmologically consistent, it will give a stringent test on SUSY models, particularly if  $\tilde{\chi}_1^0 \tilde{\chi}_1^0 \rightarrow \gamma Z$  is also observed with the correct properties. Particle Physics experiments should then provide further tests by studying neutralino production at high energy colliders, through the inverse processes  $\gamma\gamma \rightarrow \tilde{\chi}_i^0 \tilde{\chi}_j^0$  at LC and  $gg \rightarrow \tilde{\chi}_i^0 \tilde{\chi}_j^0$  at LHC. A theoretical study of these processes using the same benchmark models as in the present paper is in preparation [15].

#### Acknowledgments:

It is a pleasure for us to thank Abdelhak Djouadi for his invaluable suggestions and help, and Jean-Loïc Kneur for very helpful discussions.

## References

- [1] G. Jungman, M. Kamionkowski and K. Griest, Phys. Rep. **267**,195 (1996); M. Kamionkowski, hep-ph/0210370.
- [2] M. Drees, Pramana **51**,87(1998); M.S. Turner, J.A. Tyson, astro-ph/9901113, Rev. Mod. Phys. **71S**,145(1999); M.M. Nojiri, hep-ph/0305192; M. Drees hep-ph/0210142; J. Ellis, astro-ph/0304183.
- [3] H. Goldberg, Phys. Rev. Lett. **50**,1419 (1983); J. Ellis, J. Hagelin, D. Nanopoulos, K. Olive, M. Srednicki, Nucl. Phys. **B238**,453 (1984).
- [4] A.H. Chamseddine, R. Arnowitt and P. Nath, Phys. Rev. Lett. **49**,970 (1982); R. Barbieri, S. Ferrara and C.A. Savoy, Phys. Lett. **B119**,343 (1982); L. Hall, J. Lykken and S. Weinberg Phys. Rev. **D27**,2359 (1983).
- [5] L. Randall and R. Sundrum, Nucl. Phys. **B557**,79 (1999); G. Giudice, M. Luty, H. Murayama and R. Rattazzi, JHEP **9812**,027 (1998); J.A. Bagger, T. Moroi and E. Poppitz, JHEP **0004**,009 (2000).
- [6] M. Dine and A.E. Nelson, Phys. Rev. **D48**,1277 (1993); M. Dine, A.E. Nelson and Y. Shirman Phys. Rev. **D51**,1362 (1995); M. Dine, A.E. Nelson, Y. Nir and Y. Shirman Phys. Rev. **D53**,2658 (1996); N. Arkani-Hamed, J. March-Russel and H. Murayama, Nucl. Phys. **B509**,3 (1998); H. Murayama Phys. Rev. Lett. **79**,18 (1997); K.I. Izawa, Y. Nomura, K. Tobe and T. Yanagida, Phys. Rev. **D56**,2886 (1997); M.A. Luty Phys. Lett. **B414**,71 (1997).
- [7] H. Baer, C. Balazs, A. Belyaev, J. O'Farill, hep-ph/0305191; M. Drees and M.M. Nojiri, Phys. Rev. **D47**,4226 (1993); M. Drees and M.M. Nojiri, Phys. Rev. **D48**,3483 (1993).
- [8] D. Abrams *et.al.* [CDMS Collaboration], Phys. Rev. **D66**,122003 (2002).
- [9] R. Bernabei *et.al.* [DAMA Collaboration], Phys. Lett. **B480**,23 (2000).
- [10] L. Bergström Rep. Prog. Phys. **63**,793 (2000), hep-ph/0002126; L. Bergström and P. Ullio, Astropart. Phys. **9**,137 (1998), astro-ph/9712318; M.M. Nojiri, Pramana-journal of physics, hep-ph/0305192.
- [11] L. Bergström and P. Ullio, Nucl. Phys. **B504**,27 (1997).
- [12] Z. Bern, P. Gondolo and M. Perelstein, Phys. Lett. **B411**,86 (1997).
- [13] M. Drees, G. Yungman, M. Kamionkowski, M.M. Nojiri, Phys. Rev. **D49**,636 (1994).
- [14] L.G. Cabra-Rosetti, X. Hern/andez and R.A. Sussman, hep-ph/0302016; J. Edsjö and P. Gondolo, hep-ph/9704361, Phys. Rev. **D56**,1879 (1997).

- [15] G.J. Gounaris, J. Layssac, P.I. Porfyriadis, F.M. Renard, in preparation.
- [16] PLATON codes can be downloaded from <http://dtp.physics.auth.gr/platon/>
- [17] J. Hisano, Sh. Matsumoto and M.M. Nojiri, Phys. Rev. **D67**,075014 (2003), hep-ph/0212022.
- [18] B.C. Allanach et al, Eur. Phys. J. **C25**,113 (2002), hep-ph/0202233; G. Weiglein, hep-ph/0301111.
- [19] R. Arnowitt and B. Dutta, talk at 10th Int. Conf. on Supersymmetry and Unification of Fundamental Interactions (SUSY02), Hamburg, 2002 (hep-ph/0211042).
- [20] L. Roszkowski, talk at 37th Rencontre de Moriond on Electroweak Interactions and Unified Theories, hep-ph/0206178.
- [21] C.H. Chen, M. Drees and J.F. Gunion, Phys. Rev. **D55**,330 (1997) and (E) Phys. Rev. **D60**,039901 (1999); J. Amundson *et.al.* , Report of the Snowmass Supersymmetry Theory Working Group, hep-ph/9609374; A. Djouadi, Y. Mambrini and M. Mühlleitner, hep-ph/0104115, Eur. Phys. J. **C20**,563 (2001).
- [22] A. Djouadi, M. Drees and J.-L. Kneur, presented at "Budapest 2001 High Energy Physics Conference", hep-ph/0112026.
- [23] "SuSpect", A. Djouadi, J.-L. Kneur and G. Moultaka, hep-ph/0211331,
- [24] "HDECAY", A. Djouadi, J. Kalinowski and M. Spira, Comput. Phys. Commun. **108**,56 (1998); <http://www.desy.de/~spira/hdecay>.
- [25] D.S.Akerib, S.M. Carroll, M. Kamionkowski and S. Ritz, hep-ph/0201178. Note in particular Fig. 3 in this reference.

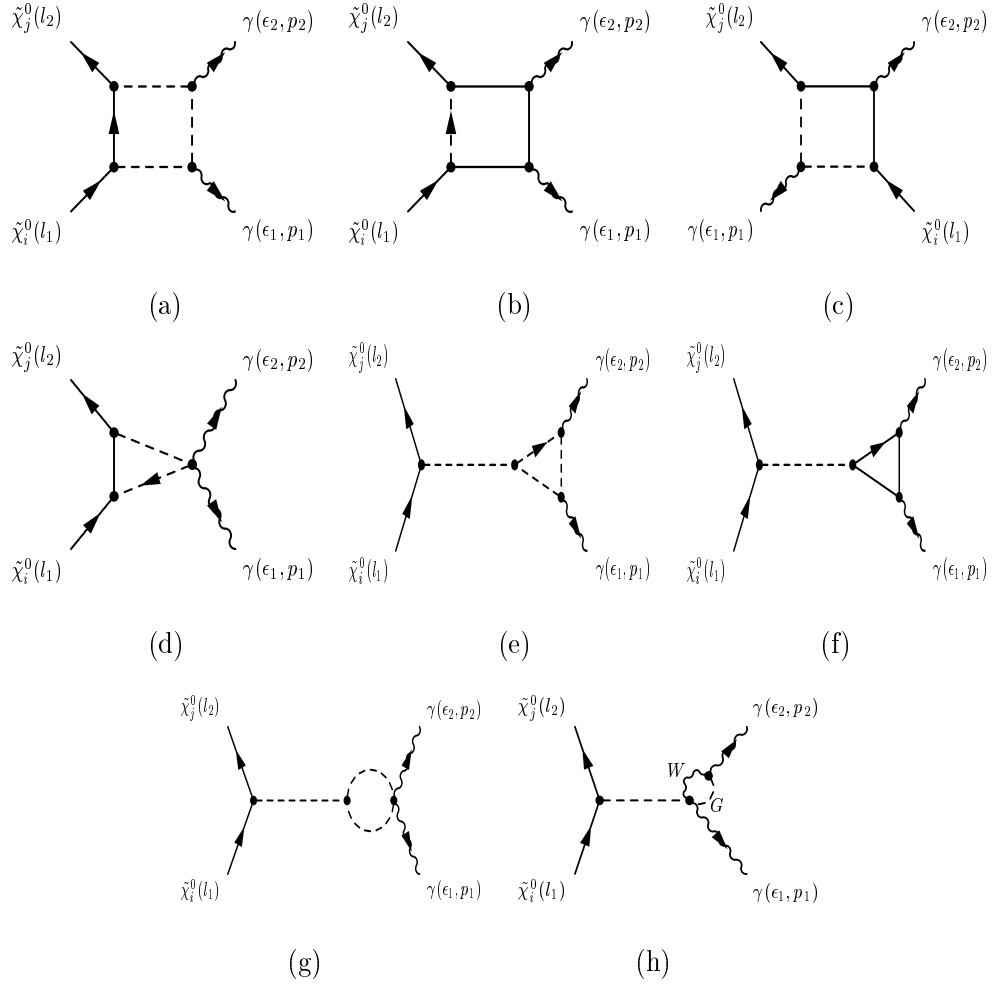


Figure 1: Feynman diagrams for  $\tilde{\chi}_i^0 \tilde{\chi}_j^0 \rightarrow \gamma\gamma$ . Full internal lines denote fermionic exchanges; while broken internal lines denote either scalar or gauge exchanges, except in the diagram (h), where the W and Goldstone exchanges are indicated explicitly.

Table 1: Universal mSUGRA Models: Input parameters are given at the grand scale, and  $v_{ij}\sigma(\tilde{\chi}_i^0\tilde{\chi}_j^0 \rightarrow \gamma\gamma, gg)$  predictions are at  $v_{ij}/c \simeq 10^{-3}$  ( $v_{ij}/c \simeq 0.5$ ).

Parameters (Dimensions in GeV)					$v_{ij}\sigma(\tilde{\chi}_i^0\tilde{\chi}_j^0 \rightarrow \gamma\gamma, gg)$ in $10^{-29} \text{cm}^3 \text{sec}^{-1}$					
$\mu > 0$					$\gamma\gamma$			$gg$		
Model	$m_0$	$m_{1/2}$	$A_0$	$\tan \beta$	$\tilde{\chi}_1^0\tilde{\chi}_1^0$	$\tilde{\chi}_1^0\tilde{\chi}_2^0$	$\tilde{\chi}_2^0\tilde{\chi}_2^0$	$\tilde{\chi}_1^0\tilde{\chi}_1^0$	$\tilde{\chi}_1^0\tilde{\chi}_2^0$	$\tilde{\chi}_2^0\tilde{\chi}_2^0$
<i>SPS5</i>	150	300	-1000	5	0.234	0.199	152.	0.0906 (0.0891)	0.689 (1.52)	8.40 (9.23)
<i>SPS1a<sub>1</sub></i>	100	250	-100	10	0.443	0.643	144.	0.460 (0.474)	0.517 (0.580)	4.40 (8.00)
<i>SPS1a<sub>2</sub></i>	140	350	-140	10	0.291	0.164	139.	0.212 (0.214)	0.205 (0.225)	10.6 (28.7)
<i>SPS1a<sub>3</sub></i>	200	500	-200	10	0.165	0.0444	134.	0.110 (0.118)	0.0342 (0.0466)	31.6 (54.3)
<i>SPS3<sub>1</sub></i>	90	400	0.	10	0.582	0.154	53.0	0.179 (0.178)	0.134 (0.173)	1553. (25.0)
<i>SPS3<sub>2</sub></i>	140	600	0.	10	0.376	0.0421	114.	0.098 (0.102)	0.0183 (0.0339)	3.36 (2.26)
<i>SPS3<sub>3</sub></i>	190	800	0.	10	0.176	0.0187	113.	0.0636 (0.0647)	0.00574 (0.0141)	1.6 (1.00)
<i>SPS2<sub>1</sub></i>	1450	300	0.	10	0.000193	0.0666	150	0.0433 (0.0470)	0.488 (0.581)	1.84 (1.80)
<i>SPS2<sub>2</sub></i>	1750	450	0.	10	0.00041	0.0112	134	0.0490 (0.0490)	0.162 (0.161)	0.611 (0.606)
<i>SPS2<sub>3</sub></i>	2050	600	0.	10	0.000265	0.00336	125	0.0207 (0.0214)	0.0585 (0.0586)	0.281 (0.280)
<i>SPS1b</i>	200	400	0.	30	0.197	0.0651	120	0.337 (0.350)	1.10 (1.40)	6.06 (4.17)
<i>AD(fg5)<sub>1</sub></i>	220	400	0.	40	0.238	0.0635	121	0.574 (0.620)	19.1 (90.6)	4.03 (3.97)
<i>AD(fg5)<sub>2</sub></i>	400	900	0.	40	0.0524	0.0153	113	0.0516 (0.0528)	10.4 (0.823)	0.814 (0.828)
<i>SPS4</i>	400	300	0.	50	0.0424	0.0685	130	5.69 (7.44)	14.7 (9.06)	7.5 (7.38)
<i>Rosz<sub>2</sub></i>	1000	1000	0.	50	0.014	0.00118	114	1.41 (0.640)	0.0341 (0.0295)	0.593 (0.597)

Table 2: Non-universal mSUGRA Models: Input parameters are given at the grand scale using dimensions in GeV and the convention  $M_2 > 0$ . In all cases  $\mu > 0$ .

	$AD(fg9)$	$SPS6_1$	$SPS6_2$	$SPS6_3$	$CDG_{200}$	$CDG_{24}$	$CDG_{75}$	$CDG_{OII}$
$M_1$	420	480	720	960	800	160	-400	424
$M_2$	420	300	450	600	160	960	240	200
$M_3$	420	300	450	600	80	-320	80	40
$m_0$	600	150	225	300	1400	1400	1400	1400
$m_{H_u}$	$600\sqrt{2}$	150	225	300	1400	1400	1400	1400
$A_0$	420	0	0	0	1000	1000	1000	1000
$\tan \beta$	40	10	10	10	50	50	50	50
$v_{ij}\sigma(\tilde{\chi}_i^0 \tilde{\chi}_j^0 \rightarrow \gamma\gamma)$ at $v_{ij}/c \simeq 10^{-3}$ in units of $10^{-29} \text{cm}^3 \text{sec}^{-1}$								
$\tilde{\chi}_1^0 \tilde{\chi}_1^0$	3.07	0.482	0.0973	0.0767	112	0.000444	0.00214	72.2
$\tilde{\chi}_1^0 \tilde{\chi}_2^0$	0.0102	7.58	1.36	0.386	7.56	0.0339	0.00488	11.3
$\tilde{\chi}_2^0 \tilde{\chi}_2^0$	14.0	115	133	133	1.64	9.66	106	1.1
$v_{ij}\sigma(\tilde{\chi}_i^0 \tilde{\chi}_j^0 \rightarrow gg)$ at $v_{ij}/c \simeq 10^{-3}$ in units of $10^{-29} \text{cm}^3 \text{sec}^{-1}$								
$\tilde{\chi}_1^0 \tilde{\chi}_1^0$	18.3	1.6	0.672	0.376	1356	0.118	2.80	13.6
$\tilde{\chi}_1^0 \tilde{\chi}_2^0$	1.34	0.986	0.514	0.427	19.8	47.6	2.82	0.425
$\tilde{\chi}_2^0 \tilde{\chi}_2^0$	1.19	5.61	12.7	3529	4.77	7.72	4.70	0.0286
$v_{ij}\sigma(\tilde{\chi}_i^0 \tilde{\chi}_j^0 \rightarrow gg)$ at $v_{ij}/c \simeq 0.5$ in units of $10^{-29} \text{cm}^3 \text{sec}^{-1}$								
$\tilde{\chi}_1^0 \tilde{\chi}_1^0$	20.0	2.00	0.811	0.455	565	0.131	2.84	11.9
$\tilde{\chi}_1^0 \tilde{\chi}_2^0$	1.39	1.62	1.42	2.39	19.0	68.5	2.50	0.407
$\tilde{\chi}_2^0 \tilde{\chi}_2^0$	1.67	9.42	2418	5.17	4.86	7.79	8.20	0.0291

Table 3: GMSB and AMSB models. Input parameters are at the big scale, and  $v_{ij}\sigma(\tilde{\chi}_i^0\tilde{\chi}_j^0 \rightarrow \gamma\gamma, gg)$  predictions are at  $v_{ij}/c \simeq 10^{-3}$  ( $v_{ij}/c \simeq 0.5$ ).

Parameters (Dimensions in GeV)				$v_{ij}\sigma(\tilde{\chi}_i^0\tilde{\chi}_j^0 \rightarrow \gamma\gamma, gg)$ in $10^{-29} \text{cm}^3 \text{sec}^{-1}$					
$\mu > 0$			$\gamma\gamma$			$gg$			
GMSB models; $n_e = n_g = N_{mes} = 3$									
Model	$M_{mess}$	$M_{SUSY}$	$\tan \beta$	$\tilde{\chi}_1^0\tilde{\chi}_1^0$	$\tilde{\chi}_1^0\tilde{\chi}_2^0$	$\tilde{\chi}_2^0\tilde{\chi}_2^0$	$\tilde{\chi}_1^0\tilde{\chi}_1^0$	$\tilde{\chi}_1^0\tilde{\chi}_2^0$	$\tilde{\chi}_2^0\tilde{\chi}_2^0$
$SPS7_1$	80000	40000	15	2.12	0.225	36.6	2.01 (2.40)	48.6 (20.9)	7.53 (6.87)
$SPS7_2$	120000	60000	15	1.15	0.124	25.5	0.409 (0.456)	7.34 (5.03)	2.61 (2.43)
$SPS7_3$	160000	80000	15	0.686	0.0545	17.4	0.146 (0.180)	2.87 (2.14)	1.04 (0.991)
$SPS8_1$	200000	100000	15	0.416	0.121	131	0.181 (0.192)	0.994 (0.947)	4.78 (8.30)
$SPS8_2$	400000	200000	15	0.119	0.00834	121	0.0299 (0.0298)	0.0457 (0.0445)	7.13 (26.9)
AMSB models									
Model	$m_0$	$m_{aux}$	$\tan \beta$	$\tilde{\chi}_1^0\tilde{\chi}_1^0$	$\tilde{\chi}_1^0\tilde{\chi}_2^0$	$\tilde{\chi}_2^0\tilde{\chi}_2^0$	$\tilde{\chi}_1^0\tilde{\chi}_1^0$	$\tilde{\chi}_1^0\tilde{\chi}_2^0$	$\tilde{\chi}_2^0\tilde{\chi}_2^0$
$SPS9_1$	450	60000	10	170	0.0355	0.487	0.229 (0.233)	0.0237 (0.0240)	0.315 (0.336)
$SPS9_2$	675	90000	10	148	0.0149	0.217	0.110 (0.112)	0.00364 (0.00374)	0.179 (0.185)
$SPS9_3$	900	120000	10	135	0.00822	0.122	0.0652 (0.0659)	0.000984 (0.00102)	0.116 (0.117)